ELSEVIER

Journal of Hazardous Materials A128 (2006) 116–121

Journal of Hazardous Materials

www.elsevier.com/locate/jhazmat

Short communication

Non-isothermal kinetics of the dehydration reaction of 3-nitro-1,2,4-triazol-5-one rubidium and cesium complexes

Haixia Ma [a,b], Jirong Song [a,*], Heming Xiao [b], Rongzu Hu [a,c], Huali Wang [a], Penggang Jin [c], Yuan Wang [c]

[a] *Department of Chemical Engineering/Shaanxi Key Laboratory of Physico-Inorganic Chemistry, Northwest University, Xi'an, Shaanxi 710069, PR China*

[b] *Department of Chemistry, Nanjing University of Science and Technology, Nanjing 210094, PR China*

[c] *Xi'an Modern Chemistry Research Institute, Xi'an, Shaanxi 710065, PR China*

Received 17 January 2005; received in revised form 17 July 2005; accepted 19 July 2005
Available online 6 September 2005

Abstract

3-Nitro-1,2,4-triazol-5-one (NTO) rubidium and cesium complexes were synthesized by mixing the aqueous solution of NTO and their respective metal carbonates. Their thermal decomposition and the non-isothermal kinetics of the dehydration reaction were studied under the non-isothermal condition by DSC and TG-DTG methods. The kinetic parameters were obtained from analysis of the DSC and TG-DTG curves by Kissinger method, Ozawa method, the differential method and the integral method. The most probable mechanism functions for the dehydration reaction of the title complexes were suggested by comparing the kinetic parameters. The dehydration decomposition reaction of $RbNTO{\cdot}H_2O$ and $CsNTO{\cdot}H_2O$ appears to be the same as Avrami–Erofeev equation: $f(\alpha) = (5/2)(1-\alpha)[-\ln(1-\alpha)]^{3/5}$, $G(\alpha) = [-\ln(1-\alpha)]^{2/5}$, $n = 2/5$. The critical temperature of thermal explosion is 240.88 °C for $RbNTO{\cdot}H_2O$ and 246.27 °C for $CsNTO{\cdot}H_2O$.
© 2005 Elsevier B.V. All rights reserved.

Keywords: 3-Nitro-1,2,4-triazol-5-one (NTO) rubidium complex; NTO cesium complex; Dehydration; Non-isothermal kinetics

1. Introduction

3-Nitro-1,2,4-triazol-5-one (NTO) is an effective, low sensitivity material with high energy [1,2]. Its metal complexes also have many special features and some potential uses in ammunition [3–10]. The impact behavior and mechanism of initiation of NTO on impact has been reported by Agrawal et al. [10] using drop-weight machine coupled with high-speed rotating mirror camera. The crystal structure of NTO salts of the heaviest alkali metals of Rb and Cs have been reported [6,11]; however, their non-isothermal kinetics of the thermal decomposition have never been studied. In this work, we reported their thermal behavior by DSC and TG-DTG techniques and studied their non-isothermal kinetics by means of Kissinger method, Ozawa method, the differential method and the integral method. This is quite useful in the evaluation of their thermal stability under non-isothermal condition and in the study of its thermal changes at high temperature for NTO salts can be a good candidate of solid propellants for suppressing the burning rate and stabilizing combustion.

2. Experimental

2.1. Sample

The NTO salt of Rb was prepared as follows: a calculated amount of Rb_2CO_3 was added gradually to the aqueous solution of NTO with stirring at 60 °C. A yellow precipitate was collected by filtration, washed with water and dried in a vacuum drier. Rb^+ was analyzed by the tetraphenylborate gravimetric method [12]. Anal. calcd. (%): C, 10.32; N, 24.09; H, 1.29; Rb, 36.77; found (%): C, 10.04; N, 23.96; H, 1.08; Rb, 36.10. The experimental results are basically con-

* Corresponding author. Tel.: +86 29 88307755; fax: +86 29 88302633.
E-mail address: dahu@nwu.edu.cn (J. Song).

0304-3894/$ – see front matter © 2005 Elsevier B.V. All rights reserved.
doi:10.1016/j.jhazmat.2005.07.054

sistent with the calculated values, so its chemical formula can be written as $Rb(C_2H_3N_4O_4)$. The characteristic peaks of IR are: $\nu^{s}_{N-H} = 3256\,cm^{-1}$, $\nu^{s}_{-OH} = 3410\,cm^{-1}$, $\nu^{s}_{C=O} = 1689\,cm^{-1}$, $\nu^{as}_{C-NO_2} = 1543\,cm^{-1}$, $\nu^{s}_{C-NO_2} = 1379\,cm^{-1}$.

The NTO salt of Cs was obtained and its component was analyzed using the same procedure as described above with Cs_2CO_3 and NTO. Cs^+ was analyzed by the same method [12] as Rb^+. Anal. calcd. (%): C, 8.57; N, 20.01; H, 1.07; Cs, 47.48; found (%): C, 8.43; N, 20.76; H, 1.03; Cs, 47.75. The characteristic peaks of IR are: $\nu^{s}_{N-H} = 3380\,cm^{-1}$, $\nu^{s}_{-OH} = 3421\,cm^{-1}$, $\nu^{s}_{C=O} = 1678\,cm^{-1}$, $\nu^{as}_{C-NO_2} = 1542\,cm^{-1}$, $\nu^{s}_{C-NO_2} = 1378\,cm^{-1}$. Its chemical formula is $Cs(C_2H_3N_4O_4)$.

2.2. Experimental equipments and conditions

The elemental analyses were performed on a PE-2400 Elemental Analytical instrument (Perkin-Elmer, USA). The infrared spectra were recorded in the 4000–400 cm^{-1} region using KBr pellets on a BRUKER EQ UNINOX-55 (BRUKER, Germany) spectrometer.

The DSC and TG-DTG experiments for the title compounds were performed using a model Q600SDT (TA, USA) under a nitrogen atmosphere at a flow rate of 150 mL min^{-1} and the amount of used sample was about 4 mg for $RbNTO{\cdot}H_2O$ and 12 mg for $CsNTO{\cdot}H_2O$. The heating rates used were 2, 5, 10, 15 and 20 °C min^{-1} from ambient temperature to 700 °C. The components of the residues are measured on a Nicolet 60 SXR FT-IR (Nicolet, USA) spectrometer in the 4000–400 cm^{-1} region using KBr.

3. Results and discussion

3.1. Thermogravimetric analysis data

DSC and TG-DTG curves of NTO, $RbNTO{\cdot}H_2O$ and $CsNTO{\cdot}H_2O$ are shown in Figs. 1–3. The exothermic peak of NTO at 275.57 °C is caused by the rapid decomposition reaction. The thermal decomposition of the two title compounds can be divided into two main stages as were observed by TG curve, and the mass loss with maximum rate was in the second stage, however in the DSC curve, there appear one endothermic and two exothermic processes which cannot be discerned clearly in the TG-DTG curve. The initial and final temperatures of the thermal decomposition process in the DSC and TG-DTG curves, the mass losses observed between these temperatures in the TG-DTG curves are showed in Table 1. It can be seen from Table 1 and Figs. 2 and 3 that the first stage of the thermal decomposition of $RbNTO{\cdot}H_2O$ and $CsNTO{\cdot}H_2O$ is connected with their dehydration processes in the temperature ranges 133.7–174.4 °C for $RbNTO{\cdot}H_2O$ and 97.0–158.2 °C for $CsNTO{\cdot}H_2O$ with mass losses of 8.15 and 6.37%. These results are in good agreement with their respective calculated values of 7.74% for $RbNTO{\cdot}H_2O$ and 6.35% for $CsNTO{\cdot}H_2O$ corresponding to the loss of 1 mol coordinated H_2O.

The degradation result can also be confirmed by the crystal structure data in Table 2. From the structure solution, the two complexes have the same coordinate number of 8 and the similar coordinate mode as shown in Fig. 4b. The center cation coordinates with two oxygen atoms on nitro-group of the first NTO anion (NTO1), one oxygen atom on a nitro-group and a

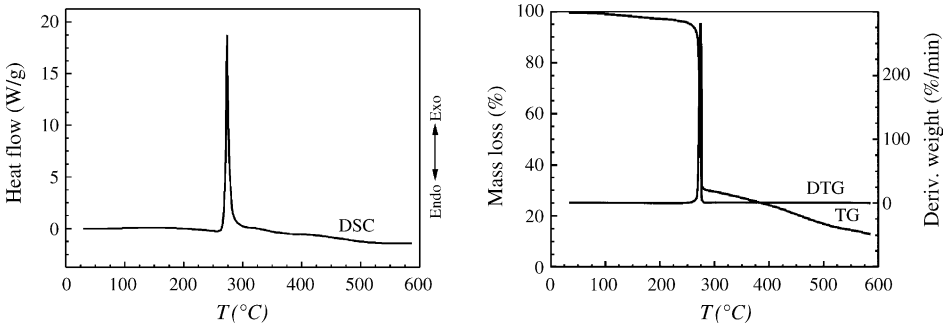

Fig. 1. DSC and TG-DTG curves of NTO at a heating rate of 10 °C min^{-1}.

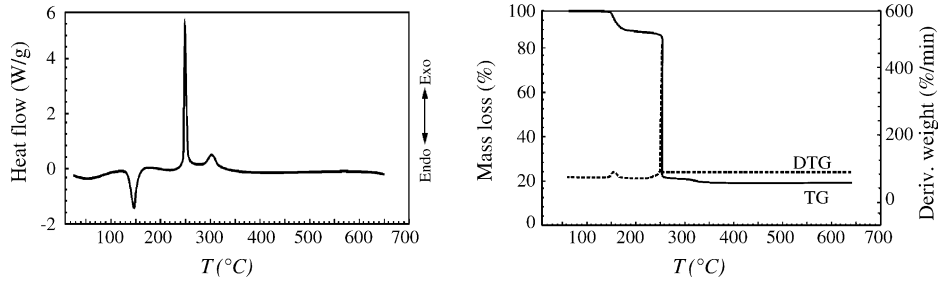

Fig. 2. DSC and TG-DTG curves of $RbNTO{\cdot}H_2O$ at a heating rate of 10 °C min^{-1}.

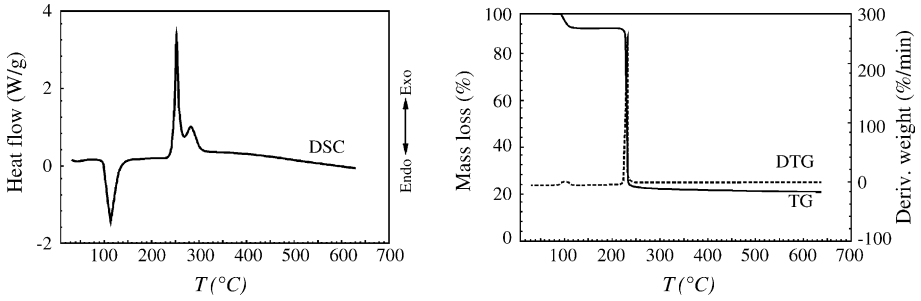

Fig. 3. DSC and TG-DTG curves of $CsNTO{\cdot}H_2O$ at a heating rate of 10 °C min^{-1}.

Table 1
Mass losses and temperature ranges of $RbNTO{\cdot}H_2O$ and $CsNTO{\cdot}H_2O$

Decomposition process	$RbNTO{\cdot}H_2O$				$CsNTO{\cdot}H_2O$			
	Mass loss (%)		T_{range} (°C)	Decomposition product	Mass loss (%)		T_{range} (°C)	Decomposition product
	Experiment	Theory			Experiment	Theory		
Stage I	8.15	7.74	133.7–174.4	RbNTO	6.37	6.35	97.0–158.2	CsNTO
Stage II	72.19		229.3–472.3	Carbonate + nitrite	70.82		219.8–439.7	Carbonate + nitrite

Table 2
The selected bond lengths of M–L

Bonds	Lengths (nm)	Bonds	Lengths (nm)
$Rb{-}O_{H_2O}$	0.2817	$Cs{-}O_{H_2O}$	0.2967
$Rb{-}O_{H_2O}$	0.2908	$Cs{-}O_{H_2O}$	0.3108
$Rb{-}O2_{NTO1}$	0.3112	$Cs{-}O2_{NTO1}$	0.3320
$Rb{-}O3_{NTO1}$	0.3319	$Cs{-}O3_{NTO1}$	0.3512
$Rb{-}O1_{NTO3}$	0.2881	$Cs{-}O1_{NTO3}$	0.3101
$Rb{-}O2_{NTO2}$	0.3007	$Cs{-}O2_{NTO2}$	0.3109
$Rb{-}O3_{NTO4}$	0.3230	$Cs{-}O3_{NTO4}$	0.3289
$Rb{-}N2_{NTO2}$	0.3151	$Cs{-}N2_{NTO2}$	0.3414

tertiary nitrogen atom on the second NTO anion (NTO2), one oxygen atom of the carbonyl on the third NTO anion (NTO3), one oxygen atom on a nitro-group on the fourth NTO anion (NTO4), two O atoms of two water molecules and these two water molecules coordinate with another cation. The selected coordinated bond lengths of $MNTO{\cdot}H_2O$ are listed in Table 2.

From the table, we can see that the bond lengths between Rb^+ and O atoms of the coordinate water molecules are 0.2817 and 0.2908 nm, shorter than those between Cs^+ and O (0.2967 and 0.3108 nm), which indicates that the coordinate bonds of $Cs{-}O_{H_2O}$ are easier to be broken down than those of $Rb{-}O_{H_2O}$ when the compound is heated.

After dehydration, the thermal decomposition of the two complexes was followed by denitrification and the ring breaking of NTO [13–16], which appears two exothermic peaks in the DSC curves. Because neither of the two processes is an independent process, there is only one process in the TG-DTG curves.

The IR spectrum of the residue at 550 °C showed that the decomposition remains was a mixture. The characteristic absorption peaks of Cs_2CO_3 and $CsNO_2$ formed at 1385 and 883 cm^{-1} and 2164 and 1255 cm^{-1}, respectively.

From the above analysis, the thermal decomposition of $RbNTO{\cdot}H_2O$ and $CsNTO{\cdot}H_2O$ can be postulated to proceed

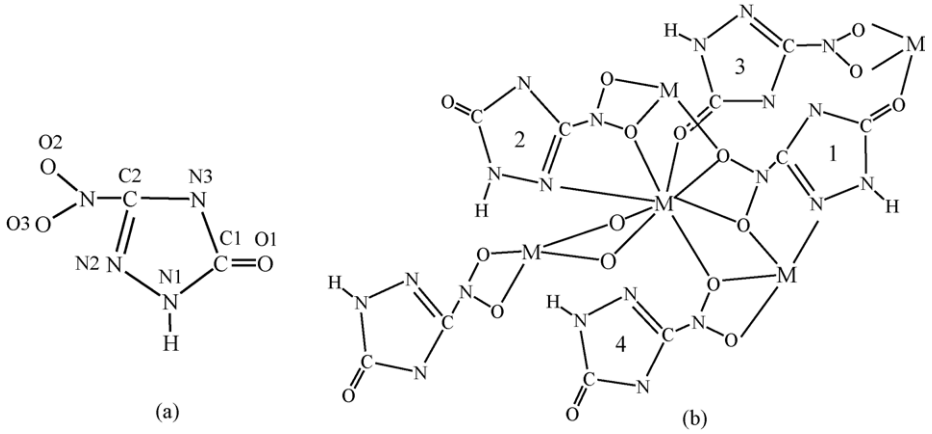

Fig. 4. The structures of NTO (a), NTO^- (b) with the atom labels in the complexes and $MNTO{\cdot}H_2O$ (M: Rb and Cs) (c).

as follows:

$$\mathrm{Rb(NTO)\cdot H_2O} \xrightarrow{133.7-174.4\,^{\circ}\mathrm{C}} \mathrm{RbNTO}$$
$$\xrightarrow{229.3-472.3\,^{\circ}\mathrm{C}} \mathrm{Rb_2CO_3 + RbNO_2}$$

$$\mathrm{Cs(NTO)\cdot H_2O} \xrightarrow{97.0-158.2\,^{\circ}\mathrm{C}} \mathrm{CsNTO}$$
$$\xrightarrow{219.8-439.7\,^{\circ}\mathrm{C}} \mathrm{Cs_2CO_3 + CsNO_2}$$

3.2. Non-isothermal decomposition kinetics

In order to obtain the kinetic parameters [apparent activation energy (E) and pre-exponential factor (A)] of the thermal decomposition of RbNTO·H_2O and CsNTO·H_2O, Kissinger equation (1) [17], Ozawa equation (2) [18], the integral equations (3)–(6) and differential equations (8)–(9) are cited to obtain the values of E, A and the most probable kinetic model function [$f(\alpha)$] from a single non-isothermal TG curve.

Kissinger equation

$$\frac{\mathrm{d}\ln\frac{\beta}{T_\mathrm{p}^2}}{\mathrm{d}\frac{1}{T_\mathrm{p}}} = -\frac{E}{R} \tag{1}$$

Ozawa equation

$$\log\beta + \frac{0.4567E}{RT} = C \tag{2}$$

Mac Callum–Tanner equation

$$\log[G(\alpha)] = \log\left(\frac{AE}{\beta R}\right) - 0.4828E^{0.4357} - \frac{0.449 + 0.217E}{0.001}\frac{1}{T} \tag{3}$$

Satava–Sestak equation

$$\log[G(\alpha)] = \log\left(\frac{A_\mathrm{s}E_\mathrm{s}}{\beta R}\right) - 2.315 - 0.4567\frac{E_\mathrm{s}}{RT} \tag{4}$$

Agrawal equation

$$\ln\left[\frac{G(\alpha)}{T^2}\right] = \ln\left\{\frac{AR}{\beta E}\left[\frac{1-2\left(\frac{RT}{E}\right)}{1-5\left(\frac{RT}{E}\right)}\right]\right\} - \frac{E}{RT} \tag{5}$$

The general integral equation

$$\ln\left[\frac{G(\alpha)}{T^2\left(1-\frac{2RT}{E}\right)}\right] = \ln\left(\frac{AR}{\beta E}\right) - \frac{E}{RT} \tag{6}$$

Achar–Brindley–Sharp equation

$$\ln\left[\frac{\mathrm{d}\alpha}{f(\alpha)\,\mathrm{d}T}\right] = \ln\left(\frac{A}{\beta}\right) - \frac{E}{RT}\left(\frac{\mathrm{d}\alpha}{\mathrm{d}t} = \beta\frac{\mathrm{d}\alpha}{\mathrm{d}T}\right) \tag{7}$$

The differential equation

$$\ln\left(\frac{\mathrm{d}\alpha/\mathrm{d}t}{f(\alpha)[E(T-T_0)/RT^2+1]}\right) = \ln\left(\frac{A}{\beta}\right) - \frac{E}{RT} \tag{8}$$

Table 3
The maximum peak temperature (T_P) of the decomposition reaction for the title compounds determined by DSC curves at various heating rates (β)

β (°C min^{-1})	RbNTO·H_2O (I)		CsNTO·H_2O (II)	
	T_{P1} (°C)	T_{P2} (°C)	T_{P1} (°C)	T_{P2} (°C)
2	131.81	238.04	97.05	244.52
5	139.52	244.94	103.89	253.78
10	148.79	255.04	113.91	263.10
15	157.76	257.17	120.95	265.75
20	159.93	262.37	122.97	269.79

where α is the fraction of conversion, dα/dt the rate of conversion at time t, T the absolute temperature at time t, T_P the peak temperature, A the pre-exponential factor, R the gas constant, E the apparent activation energy, β the linear heating rate, $f(\alpha)$ and $G(\alpha)$ the differential and integral mechanism functions, respectively, R the gas constant and C is a constant.

The values of E and A were obtained by Kissinger method (with a subscript of k) and Ozawa method (with a subscript of o) with a multiple heating method. From the original data in Table 3, the apparent activation energy E_k and E_o, pre-exponential factor A_k and linear correction coefficient r_k and r_o were determined and shown in Table 4. From the table, one can see that the rate constants at 150 °C are $10^{-1.95}$ s^{-1} for RbNTO·H_2O and $10^{-0.83}$ s^{-1} for CsNTO·H_2O which indicates the dehydration process for the latter complex is much faster than that for the former one. However, in the second stage, the rate constants at 250 °C are $10^{-1.96}$ s^{-1} for RbNTO·H_2O and $10^{-2.30}$ s^{-1} for CsNTO·H_2O, which shows the decomposition reaction for the former is faster than that for the latter.

The values of α, T and dα/dt obtained by the TG-DTG curves in Fig. 3 are listed in Table 5. By substituting the values in Tables 5 and 41 different mechanism functions $f(\alpha)$ and $G(\alpha)$ in Ref. [19] into Eqs. (3)–(7), the values of E, log A and r were obtained by the linear least-squares and iterative methods [20].

If all the following conditions are satisfied at the same time: (1) the values of E and log A obtained by differential and integral methods are approximately equal; (2) the lin-

Table 4
The kinetic parameters obtained by the data in Table 3

	RbNTO·H_2O		CsNTO·H_2O	
	First	Second	First	Second
E_k (kJ mol^{-1})	104.89	203.35	94.39	202.8
log (A_k/s^{-1})	11.00	18.32	10.82	17.95
$k_{150\,^{\circ}\mathrm{C}}$ (s^{-1})	$10^{-1.95}$		$10^{-0.83}$	
$k_{250\,^{\circ}\mathrm{C}}$ (s^{-1})		$10^{-1.96}$		$10^{-2.30}$
r_k	0.9871	0.9905	0.9887	0.9972
E_o (kJ mol^{-1})	106.37	201.64	95.82	201.2
r_o	0.9887	0.9912	0.9901	0.9975

$k_{150\,^{\circ}\mathrm{C}}$ is the rate constant at 150 °C for the title complexes and $k_{250\,^{\circ}\mathrm{C}}$ is the rate constant at 250 °C.

Table 5
Base data for MNTO·H_2O determined by TG and DTG curves

Sample no.	Data point	T (K)	α	$d\alpha/dT \times 10^3$ (K^{-1})	Data point	T (K)	α	$d\alpha/dT \times 10^3$ (K^{-1})
RbNTO·H_2O: m_s = 4.4103 mg; state, β = 10 °C min^{-1}; atmosphere, N_2, 150 ml min^{-1}; m_L = 4.0487mg; H_0 = 856.48 mJ								
I	1	408.87	0.1321	3.9656	8	416.55	0.5159	9.3319
	2	410.84	0.1961	5.0051	9	417.47	0.5844	9.6954
	3	411.80	0.2351	5.7769	10	418.40	0.6558	9.8528
	4	412.75	0.2787	6.4624	11	419.37	0.7292	9.5574
	5	413.73	0.3311	7.4008	12	420.33	0.7966	8.9853
	6	414.66	0.3870	8.0750	13	421.35	0.8604	7.640
	7	415.63	0.4504	8.7514	14	422.36	0.9100	5.9795
CsNTO·H_2O: m_s = 12.1004 mg; β = 10 °C min^{-1}; atmosphere, N_2, 150 ml min^{-1}; m_L = 11.3280 mg; H_0 = 2296.93 mJ								
II	1	372.98	0.1242	3.4418	5	380.23	0.5094	5.6772
	2	375.36	0.2313	4.4902	6	382.40	0.6438	5.8363
	3	377.98	0.3432	5.1126	7	383.88	0.7325	5.7386
	4	378.82	0.4242	5.4413	8	386.23	0.8596	5.0526

ear correlation coefficient is better; (3) the values of E and $\log A$ accord with the universal law (the value of E ranges from 80 to 250 kJ mol^{-1}, $\log A$ from 7 to 30) [20]; (4) the values of E obtained by the Ozawa method and the Kissinger method are also approximately identical with those obtained by Achar method and Mac Callum–Tanner method mentioned above, the relevant function under such conditions is the probable mechanism function of thermal decomposition of the complex. The probable kinetic model functions of the integral and differential methods selected by the logical choice method [20] and satisfying the above-mentioned conditions are $f(\alpha) = (5/2)(1-\alpha)[-\ln(1-\alpha)]^{3/5}$, $G(\alpha) = [-\ln(1-\alpha)]^{2/5}$, $n = 2/5$, indicating that the reaction mechanism of the dehydration process of RbNTO·H_2O and CsNTO·H_2O is classified as nucleation and growth and the mechanism function is no. 12, the Avrami–Erofeev equation with $n = 2/5$. The corresponding kinetic parameters are summarized in Table 6.

These values of E and A obtained from a single non-isothermal TG curve are in good agreement with the calculated values obtained by Kissinger's method and Ozawa's method. Therefore substituting $f(\alpha)$ with $(5/2)(1-\alpha)[-\ln(1-\alpha)]^{3/5}$, E with 113.06 kJ mol^{-1} for RbNTO·H_2O and 89.30 kJ mol^{-1} for CsNTO·H_2O, and A with $10^{12.08}$ s^{-1} for RbNTO·H_2O and $10^{10.32}$ s^{-1} for CsNTO·H_2O in Eq. (9)

$$\frac{d\alpha}{dt} = A\, e^{-E/RT} f(\alpha) \tag{9}$$

We can now establish the kinetic equation of dehydration reaction is

$$\frac{d\alpha}{dt} = 10^{12.48} \exp\left(\frac{-1.360 \times 10^4}{T}\right)(1-\alpha)[-\ln(1-\alpha)]^{3/5},$$

for RbNTO · H_2O,

$$\frac{d\alpha}{dt} = 10^{10.72} \exp\left(\frac{-1.074 \times 10^4}{T}\right)(1-\alpha)[-\ln(1-\alpha)]^{3/5},$$

for CsNTO · H_2O.

The value (T_{pdo}) of the peak temperature (T_p) corresponding to $\beta \to 0$ obtained by Eq. (10) taken from Ref. [21] is 229.99 °C for RbNTO·H_2O and 235.1 °C for CsNTO·H_2O.

$$T_{pdi} = T_{pdo} + b\beta_i + c\beta_i^2 + d\beta_i^3, \quad i = 1\text{–}5 \tag{10}$$

where b, c and d are coefficients.

Table 6
The kinetic parameters obtained by the data in Table 5

Sample no.	α	Equation	Mechanism function no.	E (kJ mol^{-1})	$\log(A/s^{-1})$	r
I	0.1321–0.9100	3	12	112.68	12.17	0.999994
		4	12	114.57	12.45	0.999994
		5	12	113.59	12.33	0.999994
		6	12	113.57	12.33	0.999994
		7	12	110.88	11.11	0.9916
Mean				113.06	12.08	
II	0.1242–0.8596	3	12	87.65	10.08	0.9948
		4	12	90.93	10.56	0.9948
		5	12	89.31	10.32	0.9940
		6	12	89.31	10.32	0.9972
Mean				89.30	10.32	

Function no. 12, $f(\alpha) = (5/2)(1-\alpha)[-\ln(1-\alpha)]^{3/5}$, $G(\alpha) = [-\ln(1-\alpha)]^{2/5}$, $n = 2/5$.

The critical temperature of thermal explosion (T_b) obtained from Eq. (11) taken from Ref. [21] is 240.88 °C for RbNTO·H_2O and 246.27 °C for CsNTO·H_2O.

$$T_b = \frac{E_o - \sqrt{E_o^2 - 4E_o RT_{pdo}}}{2R} \quad (11)$$

where E_o is the apparent activation energy obtained by Ozawa's method and R is the gas constant.

The entropy of activation ($\Delta S^{\#}$), enthalpy of activation ($\Delta H^{\#}$) and free energy of activation ($\Delta G^{\#}$) corresponding to $T = T_{pdo}$, $E_a = E_k$ and $A = A_k$ obtained by Eqs. (12)–(14) are 101.45 J mol^{-1} K^{-1}, 203.35 kJ mol^{-1} and 150.31 kJ mol^{-1}, respectively, for Rb(NTO)·H_2O and 94.28 J mol^{-1} K^{-1}, 202.80 kJ mol^{-1}and 154.88 kJ mol^{-1} for Cs(NTO)·H_2O.

$$A = \frac{k_B T}{h} e^{\Delta S^{\neq}/R} \quad (12)$$

$$A \exp\left(\frac{-E_a}{RT}\right) = \frac{kT}{h} \exp\left(\frac{\Delta S^{\neq}}{R}\right) \exp\left(-\frac{\Delta H^{\neq}}{RT}\right) \quad (13)$$

$$\Delta G^{\neq} = \Delta H^{\neq} - T\,\Delta S^{\neq} \quad (14)$$

where k_B is the Boltzmann constant and h is the Plank constant.

4. Conclusion

(1) The dehydration decomposition reaction of RbNTO·H_2O and CsNTO·H_2O appears to be the same as Avrami–Erofeev equation: $f(\alpha) = (5/2)(1-\alpha)[-\ln(1-\alpha)]^{3/5}$, $G(\alpha) = [-\ln(1-\alpha)]^{2/5}$, $n = 2/5$.

(2) CsNTO·H_2O is more easy to loss the compound water than RbNTO·H_2O when the complexes were heated to some temperature. However, in the second stage, the reaction speed of RbNTO·H_2O is faster than that of CsNTO·H_2O.

Acknowledgements

This investigation received financial assistance from the National Science Foundation of China (Grant 29971025) and the Backbone Teacher of Chinese University sustentation Fund of the Ministry of Education P.R. China.

References

[1] K.Y. Lee, L.B. Chapman, M.D. Coburn, J. Energy Mater. 5 (1987) 27.
[2] K.Y. Lee, M.M. Stinecipher, Propellants Explos. Pyrotech. 14 (1989) 241.
[3] J.R. Song, H.X. Ma, X.H. Sun, W. Dong, Acta Chim. Sin. 59 (2001) 1946 (in Chinese).
[4] J.R. Song, R.Z. Hu, F.P. Li, K.B. Yu, Acta Chim. Sin. 58 (2000) 222 (in Chinese).
[5] H.X. Ma, J.R. Song, X.H. Sun, R.Z. Hu, S.L. Gao, X.Y. Zhang, Thermochim. Acta 389 (2002) 43.
[6] M.C. Hu, S.Y. Gao, Z.H. Liu, J.R. Song, S.P. Xia, Chin. Sci. Bull. 46 (2001) 45.
[7] G. Singh, S. Prem Felix, J. Mol. Struct. 649 (2003) 71.
[8] G. Singh, S. Prem Felix, Combust. Flame 132 (2003) 422.
[9] G. Singh, S. Prem Felix, J. Hazard. Mater. A 90 (2002) 1.
[10] J.P. Agrawal, S.M. Walley, J.E. Field, Combust. Flame 112 (1998) 62.
[11] S.Y. Gao, M.C. Hu, S.P. Xia, T. Yue, K.B. Yu, J. Mol. Struct. 644 (2001) 181.
[12] W. Geilonann, W. Gebauhr, Z. Anal. Chem. 139 (1953) 161.
[13] J.R. Song, H.X. Ma, J. Huang, R.Z. Hu, Thermochim. Acta 416 (2004) 43.
[14] H.X. Ma, J.R. Song, R.Z. Hu, G.H. Zhai, K.Z. Xu, Z.Y. Wen, J. Mol. Struct. (Theochem.) 678 (2004) 217.
[15] H.X. Ma, J.R. Song, W. Dong, R.Z. Hu, G.H. Zhai, Z.Y. Wen, Acta Chim. Sin. 62 (2004) 1139 (in Chinese).
[16] H.X. Ma, J.R. Song, R.Z. Hu, J. Li, Chin. J. Chem. 21 (2003) 1562.
[17] H.E. Kissinger, Anal. Chem. 29 (1957) 17024.
[18] T. Ozawa, Bull. Chem. Soc. Jpn. 38 (1965) 1881.
[19] R.Z. Hu, Q.Z. Shi, Thermal Analysis Kinetics, Science Press, Beijing, 2001 (in Chinese).
[20] R.Z. Hu, Z.Q. Yang, Y.J. Liang, Thermochim. Acta 123 (1988) 135.
[21] T.L. Zhang, R.Z. Hu, Y. Xie, F.P. Li, Thermochim. Acta 244 (1994) 171.